

Zeolite Growth by Addition of Subcolloidal Particles: Modeling and Experimental Validation

Vladimiro Nikolakis,[†] Efrosini Kokkoli,[‡] Matthew Tirrell,[‡]
Michael Tsapatsis,^{*,†} and Dionisios G. Vlachos^{*,†}

Department of Chemical Engineering, University of Massachusetts–Amherst,
Amherst, Massachusetts 01003, and Materials Research Laboratory, Departments of
Chemical Engineering and Materials, University of California at Santa Barbara,
Santa Barbara, California 93106

Received October 18, 1999

Seeded growth of tetrapropylammonium (TPA)–silicalite-1 is studied using simulations and dynamic light scattering, atomic force microscopy, and transmission electron microscopy experiments. The effects of the total silica concentration, temperature, and total seed concentration are examined. When the composition of silica in solution is above a critical value, growth is observed. In such a case, the size of the seeds increases linearly with time, with a growth rate that is not significantly affected by the total silica concentration. Growth appears to be activated with an activation energy of ~ 90 kJ/mol for a range of seed concentrations. Transmission electron microscopy and dynamic light scattering indicate the presence of subcolloidal particles. Simulations of the growth of a static particle in a suspension of subcolloidal particles are carried out. Good agreement with experimental results regarding the growth rate and the apparent activation energy is possible by considering Derjaguin–Landau–Verwey–Overbeek (DLVO) interactions with electrostatic repulsion described with a constant surface charge model. The type of interaction was also verified with atomic force microscopy force measurements between a silicalite surface and a glass sphere. By use of these types of interactions, it is also possible to explain the stability of the seeded suspension and show that only a relatively narrow size distribution of growth precursors participate in the growth of the seeds. Our results support the possibility that under the conditions studied, growth of silicalite seeds proceeds by a mechanism with the rate-limiting step being the addition of subcolloidal particles.

Introduction

Despite many experimental studies on nucleation and growth of zeolites, their growth mechanism remains elusive. Elucidating the primary growth units participating in and the colloidal interactions that may affect growth of zeolite particles is an essential prerequisite for progress toward understanding the underlying mechanisms.

Experimental studies^{1,2} indicate that small colloidal particles, having sizes less than 10 nm, exist during the synthesis of several zeolite types such as Si–MFI (silicalite-1), Si–MTW, Si–BEA, and LTA. The existence of these particles has been verified for several synthesis conditions. Their size and properties are believed to be characteristic of the zeolite structure formed.^{1,3} Most of the experimental data reported in the literature exist for the tetrapropylammonium (TPA)–

silicalite-1, an all silica zeolite, and therefore, this study is focused on that system, even though the same approach can be applied to different zeolite systems.

The nucleation and growth mechanisms of silicalite-1 have been extensively studied by both small and wide-angle X-ray scattering.^{1,3–9} It has been shown⁵ that primary units (subcolloidal particles) having a size of approximately 2.8 nm are often present in the synthesis mixture independent of the structure-directing agent, alkalinity, and presence of a gel phase. In addition, these units might form small aggregates, depending on the alkalinity of the solution.^{4,5} Finally, by the use of ¹H–²⁹Si CP MAS NMR,¹⁰ preorganized inorganic–

* Corresponding authors.

[†] University of Massachusetts–Amherst.

[‡] University of California at Santa Barbara.

(1) de Moor, P.-P. E. A.; Beelen, T. P. M.; van Santen, R. A.; Tsuji, K.; Davis, M. E. *Chem. Mater.* **1999**, *11*, 36–43.

(2) Mintova, S.; Olson, N. H.; Valtchev, V.; Bein, T. *Science* **1999**, *283*, 958–960.

(3) de Moor, P.-P. E. A.; Beelen, T. P. M.; Komanschek, B. U.; Beck, L. W.; Wagner, P.; Davis, M. E.; van Santen, R. A. *Chem.–Euro. J.* **1999**, *5*, 2083–2088.

(4) de Moor, P. P. E. A.; Theo, P. M.; Beelen, T. M. P.; Komanschek, B. U.; Diat, O.; van Santen, R. A. *J. Phys. Chem. B* **1997**, *101*, 11077–11086.

(5) de Moor, P. P. E. A.; Beelen, T. M. P.; van Santen, R. A. In *Nucleation and Growth Mechanism of Zeolites: A Small-Angle X-ray Scattering Study on Si-MFI*; Materials Research Society: 1998; pp 1529–1534.

(6) de Moor, P. P. E. A.; Beelen, T. M. P.; van Santen, R. A. *Microporous Mater.* **1997**, *9*, 117–130.

(7) Dokter, W. H.; Beelen, T. M. P.; van Garderen, H. F.; Rummens, C. P. J.; van Santen, R. A.; Ramsay, J. D. F. *Colloids Surf. A* **1994**, *85*, 89–95.

(8) Dokter, W. H.; Van Garderen, H. F.; Beelen, T. P. H.; Van Santen, R. A.; Bras, W. *Angew. Chem., Int. Ed. Engl.* **1995**, *34*, 73–75.

(9) Watson, N. J.; Iton, E. L.; Keir, R. I.; Thomas, J. C.; Dowling, T. L.; White, J. W. *J. Phys. Chem. B* **1997**, *101*, 10094–10104.

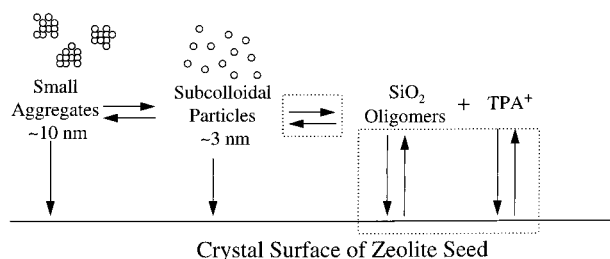


Figure 1. Possible mechanisms during growth of a silicalite crystal.

organic composite structures were found in solution during the synthesis of Si-ZSM-5. In a recent study,¹¹ silica precursor species were extracted from an aged clear synthesis suspension. The ²⁹Si CP MAS NMR data of those species were fitted to different shapes, sizes, and orientations, revealing that the best fit can be obtained for slab-shaped particles that have dimensions $1.3 \times 4.0 \times 4.0 \text{ nm}^3$. It has been speculated that these composite structures are involved in nucleation and growth through diffusion to the surface of the growing crystallites. The size of the silicalite crystals, once nucleated, is found to increase linearly with time^{4,12,13} while, at the same time, the number of the growing crystals was constant throughout the remainder of the synthesis.^{12,14}

An apparent activation energy of 70 kJ/mol of the linear growth rate has been estimated by Watson et al.⁹ using small-angle neutron scattering (SANS) and dynamic light scattering (DLS). By combining SANS and IR data, they inferred that particles of size $\sim 9.4 \text{ nm}$ can be considered as silicalite nuclei. Nucleation and growth of silicalite have also been studied by Schoeman and co-workers^{13–16} by employing several experimental techniques, including in situ DLS, Cryo TEM, Fourier transform IR spectroscopy, and so on. The observed crystal size varied linearly with time, with an apparent activation energy of $\sim 42 \text{ kJ/mol}$. On the other hand, studies using in situ DLS, under conditions similar to those reported by Schoeman et al.,¹⁷ resulted in higher apparent activation energies, in the range of 94–96 kJ/mol.¹²

Even though small subcolloidal particles have been observed with many experimental techniques, their role in nucleation and growth of silicalite-1 is still poorly understood. Experimental studies of the early stages of MFI film formation¹⁸ indicate that one of the possible nanocrystal growth mechanisms has to include transport of organic–inorganic composite species to the film surface. The possible mechanisms of TPA–silicalite-1

growth are depicted in Figure 1. An existing crystal might grow by incorporation of small subcolloidal particles (size $\sim 3 \text{ nm}$) or small aggregates of such particles ($\sim 10 \text{ nm}$) or by monomer/oligomer addition from the solution.¹⁶ At the same time, interconversions between these three “species” can take place.

In this paper, we examine the effect of colloidal interactions and different growth precursors on the growth of silicalite-1 submicrometer particles. To decouple nucleation from growth, the growth of a suspension of silicalite seeds is studied using DLS. In addition, a mathematical model is employed, for first time, to elucidate some aspects of the silicalite growth mechanisms depicted in Figure 1. More specifically, it is desired to examine whether silicalite growth by addition of subcolloidal particles is a possible mechanism. A similar mechanism for the coarsening of titania particles under hydrothermal conditions has been reported¹⁹ in the literature. In such a case, titania particles grow by oriented attachment of a small particle to a larger one with spontaneous reorganizations at the same time. It has also been mentioned¹⁹ that this mechanism is relevant to solution-mediated systems and may also be applied to systems where nucleation and coalesce on a substrate take place. The organization of this paper is as follows. First, the experimental procedure and the model are described. Next, the experimental results of the seeded growth are presented, followed by the estimation of the different parameters of the model. Finally, the modeling results are presented, followed by conclusions.

Experimental Section

The silicalite seeds and the synthesis conditions used for seeded growth are the same as the ones used for the synthesis of oriented silicalite membranes by the secondary growth method.²⁰ In brief, a suspension of silicalite seeds, with a zeolite concentration of 20 g of silicalite/L was first prepared²¹ using tetrapropylammonium hydroxide (TPAOH, 1.0 M Aldrich), fumed silica (Cab-O-Sil Grade5-M), and sodium hydroxide (NaOH, Aldrich). The resulting clear mixture of composition 10 SiO₂:2.4 TPAOH:1 NaOH:110 H₂O was placed in Teflon-lined stainless steel autoclaves and rotated in an oven at 135 °C for 3–4 h. After being cooled, a stable aqueous suspension was prepared by repeated washing with DI water and centrifuging until the pH of the sol was around 8.5. The size (diameter $\sim 80 \text{ nm}$) of the grown silicalite crystals in each suspension remains unchanged, at room temperature, over a period of several months.

The growth mixture used for the secondary growth of the seeds was prepared as follows. TPAOH (1.0 M solution, Aldrich) was mixed with distilled water. Then, a prespecified amount of tetraethyl orthosilicate (TEOS, Aldrich) was added, and the sol was stirred at room temperature for approximately 2–5 h in order to ensure complete hydrolysis of the TEOS. Eight different compositions, referred to as C1–C8 from here on, were examined and are presented in Table 1. The hydrolyzed sol was filtered with a Nalgene 0.2 μm filter in order to ensure the removal of any dust particles that might affect the DLS measurements. Small quantities of the silicalite seed suspension were added to the growth mixture by using a Drummond Scientific Company disposable 100 μL micropipet. Three different silicalite seed concentrations have been examined (0.3×10^9 , 1.9×10^9 , and 5.9×10^9 seeds/mL of soln) at solution compositions C2 and C4. The absolute values of

(10) Burkett, S. L.; Davis, M. E. *J. Phys. Chem.* **1994**, *98*, 4647–4653.

(11) Ravishankar, R.; Kirschhock, C. E. A.; Knops-Gerrits, P. P.; Feijen, E. J. P.; Grobet, P. J.; Vanoppen, P.; De Schryver, F. C.; Mieche, G.; Fuess, H.; Schoeman, B. J.; Jacobs, P. A.; Martens, J. A. *J. Phys. Chem. B* **1999**, *103*, 4960–4964.

(12) Twoney, T. A. M.; MacKay, M.; Kuipers, H. O. C. E.; Thompson, R. W. *Zeolites* **1994**, *14*, 162–168.

(13) Schoeman, B. J. *Zeolites* **1997**, *18*, 97–105.

(14) Schoeman, B. J.; Regev, O. *Zeolites* **1996**, *17*, 447–456.

(15) Schoeman, B. J.; *Microporous Mater.* **1997**, *9*, 267–271.

(16) Schoeman, B. J.; *Microporous Mesoporous Mater.* **1998**, *22*, 9–22.

(17) Schoeman, B. J.; Sterte, J.; Otterstedt, J. E. *Zeolites* **1994**, *14*, 568–575.

(18) Nakazawa, T.; Sadakata, M.; Okubo, T. *Microporous Mesoporous Mater.* **1998**, *21*, 325–332.

(19) Penn, R. L.; Banfield, F. J. *Science* **1998**, *281*, 969–971.

(20) Gouzinis, A.; Tsapatsis, M. *Chem. Mater.* **1998**, *10*, 2497–2504.

(21) Lovallo, M. C.; Tsapatsis, M. *AIChE J.* **1996**, *42*, 3020.

Table 1. Different Synthesis Solution Compositions

C1	5 SiO ₂ :9 TPAOH:9500 H ₂ O:20 EtOH
C2	10 SiO ₂ :9 TPAOH:9500 H ₂ O:40 EtOH
C3	20 SiO ₂ :9 TPAOH:9500 H ₂ O:80 EtOH
C4	40 SiO ₂ :9 TPAOH:9500 H ₂ O:160 EtOH
C5	50 SiO ₂ :9 TPAOH:9500 H ₂ O:200 EtOH
C6	60 SiO ₂ :9 TPAOH:9500 H ₂ O:240 EtOH
C7	80 SiO ₂ :9 TPAOH:9500 H ₂ O:320 EtOH
C8	120 SiO ₂ :9 TPAOH:9500 H ₂ O:480 EtOH

Table 2. Viscosity Values (in cP) at Different Composition Mixtures and Temperatures

composition	temperature °C					
	18	25	66	71	76	81
C2	1.17	1.00	0.53	0.49	0.47	0.44
C3	1.23	1.05	0.54	0.50	0.48	0.45
C4	1.34	1.15	0.57	0.52	0.50	0.47
C5	1.39	1.20	0.58	0.53	0.51	0.48
C6	1.44	1.25	0.59	0.54	0.52	0.49
C7	1.55	1.35	0.62	0.56	0.54	0.51
C8	1.77	1.55	0.67	0.60	0.58	0.55

the seed concentrations were chosen so that although there is no multiple scattering, the intensity of the scattered light is sufficiently high.

To study the growth of the silicalite seeds, their size was monitored by DLS. The sample cell assembly used is a Brookhaven Instruments BI200SM goniometer system. In this system, it is possible to control the temperature of the cell and of the matching fluid (cis-trans decahydronaphthalene). The laser source used is a Lexel 95 W Ar laser that emits vertically polarized light at 514.5 nm.

The growth of the seeds was studied at five different temperatures (66, 71, 76, 81, and 90 °C). At the lower temperatures, experiments were carried out in situ in the sample cell assembly. The temperature was controlled through a Neslab bath with external water circulation. Because it was not possible to carry out in situ experiments at 90 °C, several sample cells were placed in a preheated oven. The cells were removed and cooled to room temperature, and the particle size distribution of the suspended particles was measured by DLS. To calculate the particle size from DLS measurements, the viscosity of the suspension fluid has to be known. For that reason, viscosity measurements of the TPAOH/ethanol solutions that correspond to the total TEOS concentration have been performed at different temperatures using a precalibrated tube viscosity meter emerged in a bath. The measured values of kinematic viscosities have been converted to viscosities by using density values of the water-ethanol mixture. Finally, the data were fitted for temperature dependence at each composition, providing the values that are presented in Table 2.

The autocorrelation function was fitted with the non-negative least squares (NNLS) regression method, that can distinguish bimodal distributions. When the particle size distribution was monodisperse, the cumulants method was used to calculate the average particle size and polydispersity. On the other hand, when the distribution was bimodal, the NNLS method was used to fit the autocorrelation function.

To simulate the experimental results using the theoretical approach described, the type of interactions have to be identified and described. Atomic force microscopy (AFM) force measurements between a glass sphere and a silicalite film surface were conducted in TPABr solutions of various concentrations. The silicalite film with a surface roughness of 28–35 nm was prepared as reported in the literature.²² The measurements were performed using a NanoScope MultiMode AFM (Digital Instruments, Santa Barbara). All experiments were carried out at room temperature, and the data were converted to a force-distance curve using the method developed by Ducker et al.²³ The colloid probe tips were prepared as follows. A glass sphere (Polysciences, Inc., Warrington, PA) of radius approximately 10 μm (the radius was measured by optical microscopy) was attached to the cantilever with an epoxy resin, Epon resin 1004F (Shell Chemical, Houston, TX).

A heated thin copper wire (~30 μm diameter) attached to a three-dimensional translation stage was used to position a small portion of the glue near the apex of the cantilever. Another clean wire was used to put a glass sphere onto the tip. The cantilever was heated just enough to melt the Epon and secure the particles in place. The spring constant of the gold-coated colloid probe tips was determined using the resonant frequency method. The stiffness of the cantilevers used in the present work was in the range of 0.049–0.451 N/m.

Transition electron microscopy (TEM) of centrifuged samples, transferred on a carbon-coated grid and cooled with liquid nitrogen, was performed using the JEOL ARM-1000 operated at 800 kV at the National Center for Electron Microscopy/LBL.

Finally, a Denver Instrument Company model 50 pH/ion/conductivity meter has been used to measure conductivity after the hydrolysis of the TEOS, for estimation of the Debye-Huckel reciprocal length (see below).

Theoretical Approach

To describe growth of diluted suspensions of seeds (ideally an isolated particle), we employ a transport growth model using the Derjaguin-Landau-Verwey-Overbeek (DLVO)^{24,25} theory to account for the presence of an energy barrier to coagulation. For interacting particles performing Brownian motion, the general transport equation of the colloidal particles, with respect to a central static sphere of radius R is

$$\frac{\partial c}{\partial t} = \frac{1}{r^2} \frac{\partial}{\partial r} \left[D r^2 \frac{\partial c}{\partial r} + r^2 c \frac{D}{kT} \frac{\partial V}{\partial r} \right] \quad (1)$$

where c is the subcolloidal particle concentration, D is the diffusion coefficient of the subcolloidal particles, k is the Boltzmann constant, and V is the potential describing the effect of an externally applied force field on the mutual diffusion. In deriving the above equation, it has been assumed that (i) the superposition principle is applicable to both hydrodynamic and colloidal forces, (ii) neither temperature nor density gradients exist, and (iii) the particles are spherical, nonrotating, and isotropic.

To solve eq 1, boundary conditions have to be specified. The most common boundary condition at the surface, referred to as the *perfect sink* model,²⁶ assumes that all of the subcolloidal particles arriving at the surface of the static particle get irreversibly incorporated into it. Thus, the initial and boundary conditions are

$$\begin{aligned} c &= c_0 & r > R & & t = 0 \\ c &= 0 & r = R & & t > 0 \\ c &= c_0 & r \rightarrow \infty & & \end{aligned} \quad (2)$$

The flux of the subcolloidal particles arriving at the static particle attains a quasi-steady-state value when $t \gg R^2/D$,²⁷ which is the characteristic time for diffusion of the subcolloidal particles over a length R . The time t

(22) Xomeritakis, G.; Gouzinis, A.; Nair, S.; Okubo, T.; He, M.; Overney, R. M.; Tsapatsis, M. *Chem. Eng. Sci.* **1999**, *54*, 3521–3531.

(23) Ducker, W. A.; Senden, T. J.; Pashley, R. M. *Langmuir* **1992**, *8*, 1831–1836.

(24) Verwey, E. J. W.; Overbeek, J. T. G. *Theory of Stability of Lyophobic Colloids*; Elsevier: Amsterdam, 1948.

(25) Derjaguin, B. V.; Landau, L. *Acta Physicochim. URSS* **1941**, *14*, 733–762.

(26) Elimelech, M.; Gregory, J.; Jia, X.; Williams, R. A. *Particle Deposition & Aggregation Measurement, Modeling and Simulation*; Butterworth-Heinemann, 1995.

needed for the crystal size to increase by R is R/k_{growth} , where k_{growth} is the linear growth rate. In order for the quasi-steady-state approximation to be valid, the characteristic time for growth has to be much larger than that of diffusion. By use of typical values for the radius of the silicalite seeds and the diffusion coefficient of the subcolloidal particles, the time necessary to achieve quasi-steady-state is estimated to be of the order of milliseconds, which is much smaller than the characteristic time of growth estimated from our experiments. So the quasi-steady-state flux of the subcolloidal particles toward the central particle²⁸ is

$$J = \frac{4\pi Dc_0}{\int_{R+r_s}^{\infty} \frac{e^{-V/kT}}{r^2} dr} \quad (3)$$

where r_s is the radius of the subcolloidal particles.

It is further assumed that after the subcolloidal particles reach the crystal surface, fast local rearrangements transform the partially crystalline subcolloidal particles to the crystalline product. Because the mass rate of growth is equal to the arriving mass flux, the growth rate is

$$\frac{dR}{dt} = \frac{Dc_0(R+r_s)}{R^2 W} \frac{4}{3}\pi r_s^3 \quad (4)$$

where W is the stability ratio. In deriving eq 4, it has been assumed that the difference in densities between the subcolloidal particles and the static growing seed is negligible.

The stability ratio is a measure of the difference between the number of collisions in the absence of interactions between two particles and the actual number when interactions are taken into account. The decrease in the frequency of collisions between interacting particles compared to that for noninteracting particles performing Brownian motion is caused by an energy barrier the subcolloidal particles have to overcome before they come in contact with the growing crystallite. Because of the existence of this barrier, a growth mechanism through the addition of subcolloidal particles will appear to be activated, with an activation energy that depends on the potential used. The stability ratio is obtained from²⁶

$$W = 2 \int_0^{\infty} \frac{e^{V/kT}}{(u+z)^2} du \quad (5)$$

where $u = 2d(R+r_s)$ and d is the closest distance between the surfaces of the two particles.

To apply the above analysis to the growth of silicalite seeds, the interactions between particles have to be described. When we come to consider the long-range interactions between macroscopic particles in liquids, the two most important forces are the van der Waals and electrostatic (DLVO theory). These interactions are briefly discussed next.

Electrostatic Interactions. To calculate this force field, the Poisson–Boltzmann equation has to be solved with appropriate boundary conditions. Analytical solu-

tions can be obtained by employing several assumptions. In this study, the expressions derived assuming a constant surface potential were used first. This assumption implies that the approach of the two particles is slow and equilibrium can be established between the ions on the surface and the bulk. In addition, the surface charge distribution is assumed to be uniform, as are the solvent properties between the surfaces. The resulting expression that describes the electrostatic interactions, for relatively small surface potentials, is^{26,29}

$$V_1 = \frac{\pi\epsilon\epsilon_0 r_1 r_2 (\psi_{o1}^2 + \psi_{o2}^2)}{(r_1 + r_2)} \left[\frac{2\psi_{o1}\psi_{o2}}{(\psi_{o1}^2 + \psi_{o2}^2)} \ln\left(\frac{1 + e^{-\kappa d}}{1 - e^{-\kappa d}}\right) + \ln(1 - e^{-2\kappa d}) \right] \quad (6a)$$

where ϵ_0 is the dielectric permittivity of vacuum, ϵ is the dielectric constant of the medium, r_i is the radius of the i th particle, ψ_{oi} is the surface potential of the i th particle, and κ is the reciprocal Debye–Hückel length.

On the other hand, if the surface charge density remains constant during the approach of two particles, then a constant surface charge potential can give a better description of the interactions. The expression is similar to the one of constant potential:

$$V_1 = \frac{\pi\epsilon\epsilon_0 r_1 r_2 (\psi_{o1}^2 + \psi_{o2}^2)}{(r_1 + r_2)} \left[\frac{2\psi_{o1}\psi_{o2}}{(\psi_{o1}^2 + \psi_{o2}^2)} \ln\left(\frac{1 + e^{-\kappa d}}{1 - e^{-\kappa d}}\right) - \ln(1 - e^{-2\kappa d}) \right] \quad (6b)$$

It should be mentioned that the two cases described above are extremes, and the real behavior of particle surfaces could be somewhere in between.

van der Waals Interactions. The van der Waals interaction between two bodies has been calculated by Hamaker, who assumed pairwise additivity of the interactions of all individual molecules. The expressions describing the interactions of two macroscopic bodies consist of two parts. The first one describes the geometry of the system. The second one describes the properties (e.g., limiting refracting index and characteristic dispersion frequency) of the interacting bodies and the medium and is taken into account in the value of the Hamaker constant. Because of the assumption of pairwise additivity of all intermolecular forces, the potential calculated with this approach is overestimated. An expression that gives the van der Waals interaction between two particles is²⁶

$$V_2 = -\frac{A}{6} \left(\frac{2r_1 r_2}{d^2 + 2r_1 d + 2r_2 d} + \frac{2r_1 r_2}{d^2 + 2r_1 d + 2r_2 d + 4r_1 r_2} + \ln\left(\frac{d^2 + 2r_1 d + 2r_2 d}{d^2 + 2r_1 d + 2r_2 d + 4r_1 r_2}\right) \right) \quad (7)$$

where A is the effective Hamaker constant.

(27) Levich, V. G. *Physicochemical Hydrodynamics*; Prentice Hall, Inc., Englewood Cliffs, N. J., 1962.

(28) Fuchs, v. N. *Z. Physik* **1934**, *89*, 736–743.

(29) Hogg, R.; Healy, T. W.; Fuerstenau, D. W. *Trans. Faraday Soc.* **1966**, *62*, 1638–1651.

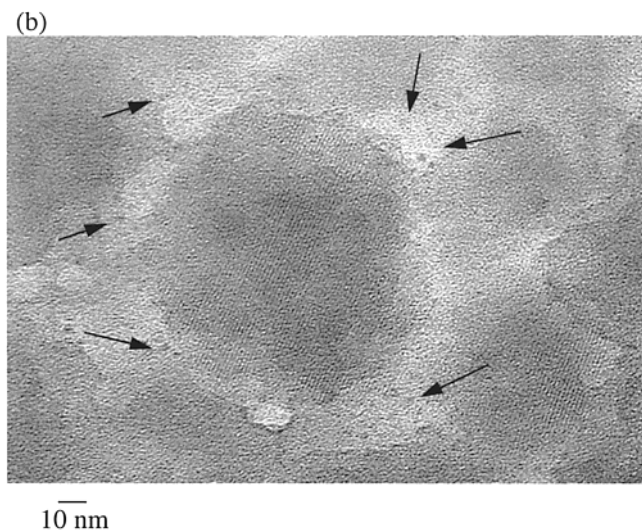
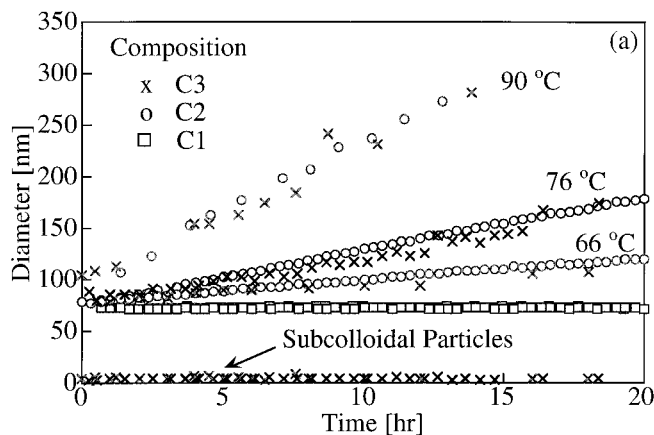


Figure 2. (a) Changes of the size of TPA-silicalite-1 seeds with time for different temperatures and solution compositions listed in Table 1 (for composition C1 the points for all temperatures coincide). (b) TEM image of silicalite crystal, showing the existence of particles having size 2–3 nm in its vicinity.

The above expressions of the interparticle potentials were derived from the corresponding ones for two flat, infinite surfaces using the Derjaguin approximation.³⁰ This approximation is accurate for any type of potential as long as the separation distances of the spheres are much smaller than their radii. As will be shown later, most of the changes in the potential take place at interparticle distances less than 2 nm, which are much smaller than the size of the seeds and comparable to the size of the subcolloidal particles.

Results and Discussion

DLS Measurements. The seeds prepared had an effective diameter of ~ 80 nm, and their polydispersity was very small (~ 0.01), both as analyzed by DLS. Their size and monodispersity were also examined by SEM images of seeds deposited on alumina substrates and found to be in good agreement with the DLS results.

Figure 2a shows the results for three different initial silica compositions (C1–C3) in solution at three different temperatures (for clarity, the data for the temper-

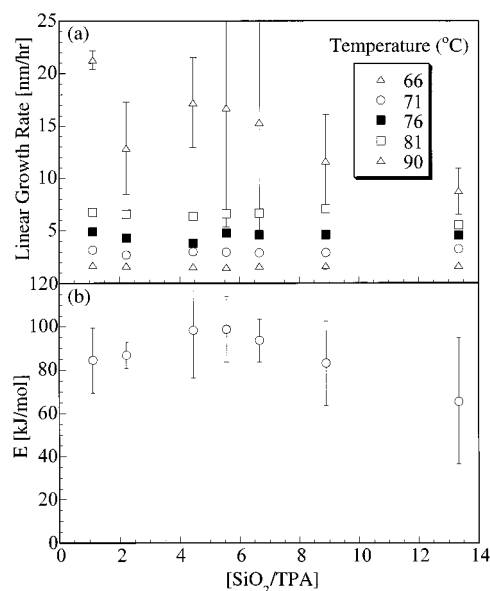


Figure 3. (a) Comparison of linear growth rates as a function of composition. (b) Comparison of activation energies of growth for different solution compositions.

atures 71 and 81 °C are not presented in the graph), for a seed concentration of 1.5×10^9 seeds/mL. The various compositions are marked with different symbols. When a small amount of TEOS (composition C1) was hydrolyzed, the size of the silicalite seeds remains unchanged during the time of the observation, indicative of a near-equilibrium situation. DLS was not able to distinguish a second particle distribution of subcolloidal particles. The same behavior was observed for all temperatures examined. When the total amount of silica is increased (compositions C2–C8), growth takes place. A population of small subcolloidal particles has been observed for the higher total silica concentrations (compositions C3–C8). Evidence for the existence of small particles 2–3 nm can also be seen in the TEM image shown in Figure 2b. The representative micrograph shows subcolloidal particles with size 2–3 nm in the vicinity of a growing silicalite.

The crystal size increases linearly with time and seems to practically be independent of the total silica content of the solution (Figure 3a). The scattering of the data at 90 °C is larger because the experiments were performed ex situ. The error bars of the measurements at the lower temperatures are of the same size as the symbols and are not shown in the figure.

The fact that no subcolloidal particles have been detected during the synthesis with composition C2 is possibly due to the inability to resolve a bimodal distribution when the relative size of one of the peaks is too low. This is also supported by the fact that for the same synthesis composition (C2) it was possible to observe the subcolloidal particles at smaller seed concentrations (e.g., 0.3×10^9 seeds/mL). In the latter case, the relative value of intensity of the scattered light due to the presence of the subcolloidal particles is larger, making their detection possible.

The average effective diameter of the subcolloidal particles, as analyzed by DLS, fluctuates between 2.5 and 5 nm, with a distribution around the mean value of the order of 1 nm. These fluctuations also seem to be

(30) Israelachvili, J. *Intermolecular & Surface Forces*; Academic Press: 1991.

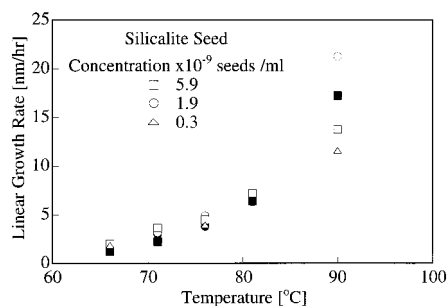


Figure 4. Comparison of linear growth rates vs temperature for experiments performed at different silicalite seed concentrations. The open symbols correspond to composition C2 and the filled ones to C3.

temperature-independent. The observed sizes of the subcolloidal particles are in good agreement with several reported literature values.

Growth is activated for compositions C2–C8 (Figure 3b). The corresponding values of the apparent activation energies, shown in Figure 3b, are within the range of 70–120 kJ/mol, consistent with most literature data reported.

In addition to the effect of the total silica concentration on growth rate, the effect of the silicalite seeds was also examined. Measurements for different silicalite seed concentrations have been carried out, revealing similar behavior. Figure 4 shows the measured linear growth rates for all of the different conditions examined. Growth experiments at higher and lower seed concentrations are not feasible due to multiple scattering and the low intensity of the scattered light, respectively.

Parameter Estimation. To simulate the experimental results using the theoretical approach described, the interactions listed above have to be specified. Even though the AFM force measurements were performed at nonreactive conditions significantly different from the ones used in the growth experiments, they can reveal information about the type of interactions taking place. Figure 5a presents the normalized force curves (with the radius of the sphere) at different TPABr concentrations. The data were fitted for surfaces interacting at both constant surface charge and constant surface potential, but they were more consistent with an interaction based on the former boundary condition (Figure 5b). These fits give an estimation of the surface potential and the Hamaker constant, parameters necessary to describe the interparticle interactions. The fitted values of Hamaker constant and surface potential are significantly affected by the concentration of TPABr. The value of Hamaker constant reduces from 4.5×10^{-20} J, when no TPABr is added to the solution, to 3×10^{-21} J when $[\text{TPABr}] = 0.05$ M. Furthermore, the absolute value of the fitted surface potential decreases by increasing the TPABr concentration from -40 to -7 mV at neutral pH, indicating increased ion binding or screening of the double-layer repulsion. This behavior is in agreement with ζ -potential measurements.

The ζ -potential of silicalite-1 crystals at high pH values (>10) is found to be constant with a value of about -50 mV.³¹ The pH at the synthesis conditions is

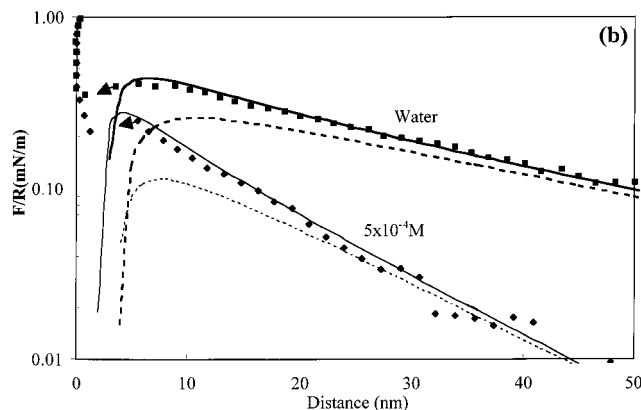
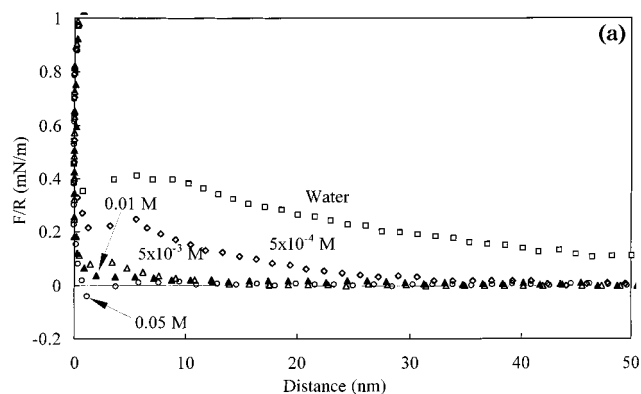


Figure 5. (a) Normalized force curves (with the radius of the sphere) between a $19.76 \mu\text{m}$ glass sphere and a silicalite surface, for various TPABr concentrations. (b) Semilog graph of the normalized forces for two concentrations along with the DLVO fits. The arrows in part b indicate a jump into an adhesive minimum. The solid lines are the fit to DLVO theory at constant surface charge, and the dashed lines are the fit for constant surface potential.

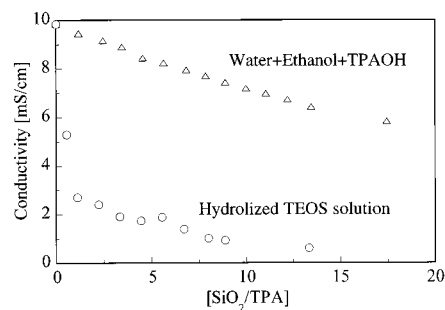


Figure 6. Conductivity changes as a function of composition.

~ 11.9 , and therefore, the reported value of -50 mV is used in the simulations.

The Debye–Huckel reciprocal length can be calculated by taking into account the total concentrations of the various ions added to the system. A problem with this approach is that the fraction of free ions in the solvent is not known. As mentioned earlier, the TPA cations get entrapped in composite organic–inorganic structures, reducing the amount of TPA ions that are free in the solution. To resolve this issue the conductivity of the hydrolyzed TEOS solutions and of solutions having equivalent amounts of water, ethanol, and TPAOH were measured. The conductivity of the TPAOH solution was ~ 10 mS/cm, and it decreases linearly with the amount of ethanol added to the system (Figure 6). Similar behavior has been observed when measuring

(31) Persson, A. E.; Schoeman, B. J.; Sterte, J.; Otterstedt, J.-E. *Abstr. Papers Am. Chem. Soc.* **1995**, 159–173.

Table 3. Debye–Huckel Reciprocal Lengths Calculated from Conductivity Data at 25 °C

[TEOS]	κ^{-1} (nm)	[TEOS]	κ^{-1} (nm)
0	1.43	50	3.20
5	1.94	60	3.71
10	2.71	70	4.33
20	2.86	80	4.49
30	3.20	120	5.49
40	3.34		

the conductivity at the end of the TEOS hydrolysis for different TEOS concentrations (Figure 6). The decrease is not linear with the amount of TEOS added, and the absolute values are much smaller than the corresponding values of the water/ethanol/TPAOH solution. This is in qualitative agreement with the argument that TPA ions get entrapped in the subcolloidal particles, whose number decreases by decreasing the total concentration of silica (see below). Given the conductivity σ of the medium, the Debye–Huckel reciprocal length can be estimated from the following equation³²

$$\kappa^2 = \frac{\sigma}{\epsilon_0 \epsilon D_{\text{ion}}} \quad (8)$$

where D_{ion} is the average ionic diffusivity calculated from the corresponding values of TPA^+ and OH^- at 25 °C.³³ The values of the Debye–Huckel reciprocal length estimated from eq 11 for compositions C1–C8 are presented in Table 3.

The dielectric permittivity of the medium was calculated from water and ethanol dielectric permittivity data,³⁴ following mixing rules described in the literature.³⁵

Simulation Results. The growth of a static crystal was first simulated for noninteracting particles and next for interacting particles with several variations of the classic DLVO theory. For the latter case, both the constant charge and constant potential electrostatic interactions were examined. For each model case, the different model parameters were independently varied within the limits of experimental uncertainty or within the literature reported ranges. The results for the different types of interactions are presented next.

Noninteracting Particles. Simulations for the case of noninteracting particles (only diffusion as a driving force) show that it is not possible to explain any of the experimentally observed features regarding seeded growth of silicalite (e.g., linear growth rate, activation energies, stability of seeds).

Constant Surface Potential. By describing the interparticle interactions with a constant surface potential model, it was not possible to get good agreement with the experimentally estimated activation energies unless unrealistic values of parameters (e.g., too high ζ -potential or Hamaker constant value) were used.

Constant Surface Charge. Our simulations indicate that it is possible to achieve good agreement with the experimental data by using the constant surface charge

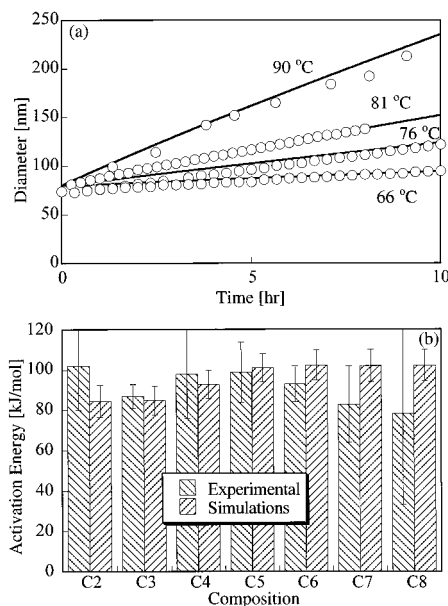


Figure 7. (a) Comparison of experimentally measured growth curves of TPA–silicalite-1 seeds with simulated ones for composition C3. (b) Activation energies for various compositions. The simulation parameters are $\psi_0 = -50$ mV, $A = 1.5 \times 10^{-20}$ J, diameter of subcolloidal particles = 2.8 nm, and diameter of seeds = 80 nm. The concentrations of subcolloidal particles used are 0.33, 0.33, 1.0, 1.5, 1.5, 2.2, 2.8×10^{-12} cm⁻³ for compositions C2–C8, respectively.

potential. The size of the subcolloidal particles was fixed to the one that is most often reported in the literature.^{1,3,9,15} $d_s = 2.8$ nm. This value is within the range of subcolloidal particle sizes measured in our DLS experiments. The Hamaker constant was varied within the acceptable range of values in order to fit the experimental activation energies. The value that was finally used was 1.5×10^{-20} J and was kept constant for all compositions and temperatures. The bulk concentration of subcolloidal particles was also varied in order to fit the value of the simulated growth rate to the experimental ones. As can be seen from eqs 4 and 5, the subcolloidal particle concentration does not affect the apparent activation energy. Good agreement with the experimental results can be achieved when the concentration is on the order of 10^{12} cm⁻³.

Assuming that all the silica, after the hydrolysis of TEOS, is transformed to subcolloidal particles with a diameter of 2.8 nm, will result in a particle concentration on the order of 10^{17} cm⁻³, which is orders of magnitude larger than the one that fits the data. As mentioned in the Introduction, experimental observations^{1,3,36} indicate that the subcolloidal particles coexist with a second population of aggregates of diameter ~ 10 nm. A relatively small concentration of aggregates ($\sim 10^4$ cm⁻³) can explain why the fitted value of subcolloidal particle concentration is much smaller. As will be explained later, these aggregates do not contribute significantly to growth.

In Figure 7a, the experimental results are compared with the simulation ones for composition C3, at four different temperatures. Despite the variation of the model input parameters (κ , ϵ) (the error bars indicate

(32) Bogush, G. H.; Zukoski IV, C. F. *J. Colloid Interface Sci.* **1991**, *142*, 19–34.

(33) Cussler, E. L.; *Diffusion Mass Transfer in Fluid Systems*; Cambridge University Press: 1997.

(34) *Handbook of Chemistry and Physics*, 1st student ed.; CRC Press: Boca Raton, FL, 1988.

(35) Petit, J.-M.; Law, B. M.; Beysens, D. *J. Colloid Interface Sci.* **1998**, *202* 441–449.

(36) de Moor, P.-P. E. A.; Beelen, T. P. M.; Komanschek, B. U.; van Santen, R. A. *Microporous Mesoporous Mater.* **1998**, *21*, 263–269.

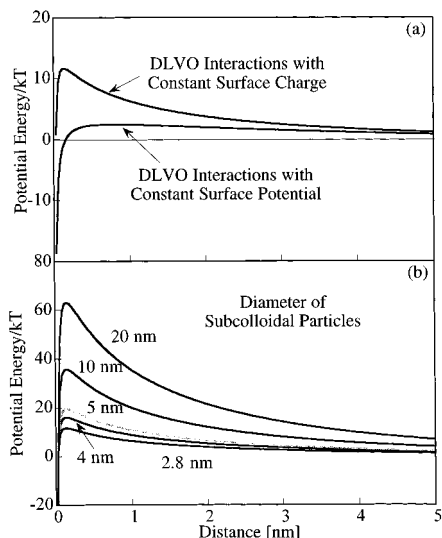


Figure 8. (a) Total potential energy between a subcolloidal particle of 2.8 nm in diameter and a 80 nm silicalite seed vs their closest distance. (b) Dependence of the interparticle potential on the diameter of subcolloidal particles. The rest of the simulation parameters are the same as ones described in Figure 7.

the standard deviation due to fitting of growth rate curves in an Arrhenius graph), Figure 7b depicts a very good agreement between the calculated and the experimental activation energies. This result shows that over the range of the compositions (C2–C8) examined the activation energies are practically independent of composition. The activation energy was calculated from the fitted linear growth rates of the simulation results. These results strongly indicate that association of subcolloidal particles with the crystal, followed by fast rearrangements on the crystal surface, is a possible mechanism of silicalite growth. In such a case, the apparent activation energy observed during the silicalite growth can be attributed to the repulsion that is caused by the overlap of the electrical double layers of the silicalite seeds and the subcolloidal particles as they approach each other. The constant charge or constant potential approximations that have been used are the two limiting cases for the interactions, but they constitute a good first approximation when no detail information about the surface behavior is available. To examine the qualitative differences between the various potentials, Figure 8a compares the shape and maximum of the potential for the classic DLVO (constant charge and constant potential) interactions for the same values of parameters. It can be seen that according to the constant potential DLVO theory a small maximum in the potential energy is present. On the other hand, the constant charge DLVO theory gives a higher potential barrier.

Another experimental observation that can be explained by this model is the observed stability of the silicalite seeds suspension. When the size of the growth units is taken to be as large as that of the silicalite seeds while the rest of the parameters remain the same, the size of the static seed remains unchanged during the simulation. An increase in the size of the growth units (subcolloidal particles) results in an abrupt rise of the potential maximum as shown in Figure 8b. The increase of the potential maximum is a geometric effect described

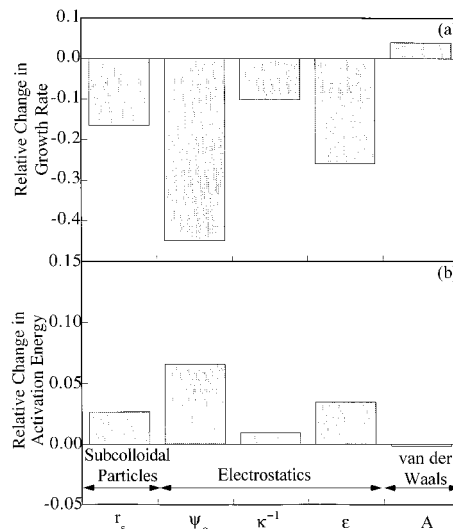


Figure 9. Normalized sensitivity coefficients over the nominal values of growth rate and activation energy with respect to model parameters. The perturbation introduced in each parameter is 2%.

by the term $r_1 r_2 / (r_1 + r_2)$ of eq 6. Consequently, a suspension of larger crystals appears to be stable because the energy barrier that the particles have to overcome for agglomeration is larger.

An important implication of the strong dependence of the interaction potential on subcolloidal particle size is the large sensitivity of the growth rate and activation energy on the subcolloidal particle diameter. In particular, we have found that only a relatively narrow subcolloidal particle size distribution (up to ~ 4 nm in diameter) can result in reasonable growth rates and activation energies. For example, small subcolloidal particles result in very fast growth and very low activation energy. Conversely, large aggregates of subcolloidal particles give low growth rates and large activation energies. This indicates that possible aggregates of subcolloidal particles, depicted in Figure 1, are not directly consumed in the growth of an already existing crystal, and consequently, the smallest existing subcolloidal particles have the largest contribution to the growth.

As has been mentioned earlier, the total silica concentration affects the Debye–Huckel reciprocal length. At the same time, the total amount of ethanol changes because a different amount of TEOS is hydrolyzed, causing a change in the dielectric constant of the medium. These changes are already captured in the model. On the other hand, the surface potential and the Hamaker constant have not been directly measured and are not varied with composition. It is desired to examine the effect of the uncertainty of each parameter in the results. Sensitivity analysis of the growth rate and activation energy with respect to the various model parameters, shown in Figure 9, indicates that the surface potential value can significantly affect both the growth rate and activation energy. So it is very important to have an accurate description of the surface properties and behavior as the two particles approach each other.

The stability of a suspension of subcolloidal particles has also been examined by considering a static particle of a small diameter, e.g., equal to that of the subcolloidal

particles. In such a case, the size of the static particle increases with time. This implies that in the absence of a dissolution mechanism, subcolloidal particles will agglomerate, forming bigger particles. This result indicates that there may be a competition between the addition of the subcolloidal particles to the already existing crystals and their agglomeration toward the formation of a second population of larger particles. To capture these issues, more detailed information about the formation and dissolution of the subcolloidal particles has to be included in the model.

Conclusions

Seeded growth of TPA-silicalite-1 seeds was studied using dynamic light scattering as the primary experimental technique. The effect of the total silica concentration, temperature, and total seed concentration was examined. At high concentrations of silica in the solution, growth is observed, with a linear growth rate that is practically independent of the total silica added to the system. Growth is activated with an activation energy of ~ 90 kJ/mol, which is independent of the silica concentration. The seed concentration over the range (0.1×10^9 – 5.9×10^9 seeds/cm³ of soln) does not affect the above conclusions.

TEM results support the presence of ~ 3 nm subcolloidal particles in the vicinity of the growing seeds.

To understand the experimental observations, the growth rate of silicalite seeds was determined through modeling of a static particle in a suspension of subcolloidal particles. Good agreement with experimental

results regarding the growth rate and activation energy is possible considering DLVO interactions under a constant surface charge. The constant surface charge model is supported by AFM measurements. With this model, it is also possible to explain the stability of the seeded suspension and understand why the smaller subcolloidal particles (diameter ~ 2.8 nm) are more likely the ones contributing to the growth. Our results support a mechanism where the rate-limiting step for growth of silicalite is the addition of subcolloidal particles.

Acknowledgment. We acknowledge instrumentation support from the National Science Foundation (CTS-9410994 and CTS 9904242) and the Department of Defense (DURIP). D.G.V. and M.Tsapatsis acknowledge support from the National Science Foundation (CAREER, CTS-9702615, and CAREER, CTS-9612485) and NETI. M.Tsapatsis acknowledges support from a David and Lucille Packard Foundation Fellowship in Science and Engineering, as well as a Camille and Henry Dreyfus Teacher-Scholar Award. TEM was performed on the National Center for Electrical Microscopy at Laurence Berkeley Laboratory under a 1995 NCEM/DOE Fellowship to M.Tsapatsis. M.Tirrell and E. K. acknowledge support from the National Science Foundation (CTS-9616797) and the Center for Interfacial Engineering at the University of Minnesota for the use of their characterization facility.

CM990653I